Charge transfer rates in organic semiconductors beyond first-order perturbation: From weak to strong coupling regimes

Guangjun Nan, Linjun Wang, Xiaodi Yang, Zhigang Shuai, and Yi Zhao

Citation: The Journal of Chemical Physics **130**, 024704 (2009); doi: 10.1063/1.3055519
View online: https://doi.org/10.1063/1.3055519
View Table of Contents: http://aip.scitation.org/toc/jcp/130/2
Published by the American Institute of Physics

Charge transfer rates in organic semiconductors beyond first-order perturbation: From weak to strong coupling regimes

Guangjun Nan,[1] Linjun Wang,[1] Xiaodi Yang,[1] Zhigang Shuai,[2,1,a)] and Yi Zhao[3]
[1]*Key Laboratory of Organic Solids, Beijing National Laboratory for Molecular Sciences (BNLMS), Institute of Chemistry, Chinese Academy of Sciences, 100190 Beijing, People's Republic of China*
[2]*Department of Chemistry, Tsinghua University, 100084 Beijing, People's Republic of China*
[3]*State Key Laboratory of Physical Chemistry of Solid Surfaces and Department of Chemistry, Xiamen University, 361005 Xiamen, People's Republic of China*

(Received 20 August 2008; accepted 26 November 2008; published online 12 January 2009)

Semiclassical Marcus electron transfer theory is often employed to investigate the charge transport properties of organic semiconductors. However, quite often the electronic couplings vary several orders of magnitude in organic crystals, which goes beyond the application scope of semiclassical Marcus theory with the first-order perturbative nature. In this work, we employ a generalized nonadiabatic transition state theory (GNTST) [Zhao *et al.*, J. Phys. Chem. A **110**, 8204 (2004)], which can evaluate the charge transfer rates from weak to strong couplings, to study charge transport properties in prototypical organic semiconductors: quaterthiophene and sexithiophene single crystals. By comparing with GNTST results, we find that the semiclassical Marcus theory is valid for the case of the coupling <10 meV for quaterthiophene and <5 meV for sexithiophene. It is shown that the present approach can be applied to design organic semiconductors with general electronic coupling terms. Taking oligothiophenes as examples, we find that our GNTST-calculated hole mobility is about three times as large as that from the semiclassical Marcus theory. The difference arises from the quantum nuclear tunneling and the nonperturbative effects.
 [DOI: 10.1063/1.3055519]

I. INTRODUCTION

Charge transport in organic semiconductors has been a subject of fundamental interest for decades,[1] but the precise nature of charge carrier transport has not been fully resolved yet.[2,3] The realizations of electronic and optoelectronic devices trigger a renewed interest in better understanding the intrinsic charge transport processes.[4] Recently, new techniques developed for preparing ultrapure single crystals of these organic materials provide a useful tool to achieve this goal. A number of experimental and theoretical studies have shown that the mechanisms of charge transfer (CT) in organic conductive materials are subject to considerable uncertainties and likely differ substantially for different materials.[5–9] Among these, thiophene-based materials are a promising class of organic materials for their use in organic thin film transistor.[10] In order to estimate the full potentials of these materials, a better understanding of the intrinsic charge transport mechanism is needed.

It turns out that, at low temperatures, the charge transport in a number of organic crystals can be described in a bandlike regime.[11] As the temperature increases, the dynamic structure disorder may invalidate the band transport model. This leads to a high temperature regime where the charge carriers get localized over single molecule and transport behavior is governed by a thermally activated hopping mechanism.[2,6,12] Semiclassical Marcus hopping model[13] for self-exchange charge transfer processes has been widely employed, as follows:

$$k_{\mathrm{Marcus}} = \frac{|t|^2}{\hbar}\sqrt{\frac{\pi}{\lambda k_B T}}\exp(-\lambda/4k_B T), \tag{1}$$

where k_B denotes the Boltzmann constant and T is the temperature. Equation (1) indicates that the rate of CT depends on two main parameters: the reorganization energy λ and the electronic coupling t. These molecular parameters greatly help in designing organic semiconductors.[5,14,15] At this stage, however, it is worth stressing that this formula implies that the system has to reach a transition state for the CT to occur.

Recently, several experiments performed on organic single crystals have made clear that this model is inadequate. For example, ultrapure single crystals of pentacene and rubrene show a "bandlike" mobility,[8,16] but the analysis of experimental data indicates that a mean free path of the charge carriers is close to the distance between molecules,[17] a fact that is in sharp contrast to a delocalized picture. To explain this seeming contradiction, Troisi and Orlandi[18,19] argued that the thermal molecular motions in organic crystals may cause large fluctuations in the intermolecular transfer integrals, which can localize the charge carrier and reduce the mobility. This description excluded the bandlike picture and explained temperature dependence at the same time. Since the conjugated CC stretching modes are ~ 1500 cm^{-1}, the classical high temperature limit assumed in Eq. (1) is only approximate and quantum motion of nucleus should be con-

a)Electronic mail: zgshuai@tsinghua.edu.cn.

sidered. Based on this point, the present authors have shown that a full quantum mechanical Fermi golden rule (FGR) treatment[20] would largely lower the actual barrier from that computed from λ as described in Eq. (1), which leads to a bandlike mobility behavior for rubrene single crystals within the hopping model.[21]

In spite of the popularity of Eq. (1) due to its simplicity and the clear physical meanings of the two parameters, this formalism is based on the perturbation theory and is limited to the high temperature case. In actual organic crystals, electronic couplings can be large in some directions compared to the reorganization energy, which makes Eq. (1) invalid. When the coupling is large enough, i.e., in adiabatic limit, the reactions may be controlled by the motion on the lower adiabatic potential energy surface (PES) and the activation rate theory[22] can be applied. However, the calculation of the rates in the "crossover region" where the electronic coupling term changes from the weak to the strong regions, still presents a considerable challenge.[23] Numerous attempts on the basis of nonadiabatic transition state theories[24–26] (NA-TSTs) have been developed to incorporate these two limits in a consistent and uniform way.

In most NA-TSTs, the nonadiabatic transition probability is frequently manipulated by the Landau–Zener (LZ) formula[27] for the two-state curve crossing problem. However, it is well known that the LZ theory does not work in the region where the kinetic energies are near or lower than the crossing point, i.e., it does not incorporate the nonadiabatic nuclear tunneling, and it neglects the coupling effect of the electronic and nuclear tunnelings. Besides, the LZ probability is not very accurate for the case of strong diabatic coupling. Later, Zhu and Nakamura (ZN) proposed a new nonadiabatic transition probability[28] which is practically free from the above drawbacks. It completely covers the whole energy region in two-state curve crossing problem and can be implemented by only using information of the adiabatic PESs.

In a nonadiabatic chemical process, it is very difficult to carry out a rigorous quantum mechanical rate constant for multidimensional CT problems. Thus, some useful semiclassical methods are required to be developed. Recently, Zhao *et al.* combined the flux-side correlation function[29] and the ZN formulas[28] to derive a semiclassical generalized NA-TST formula for rate constants.[30–32] In their work, a general seam surface was taken into account, which led to a better result than that from taking only minimum energy crossing point[25] at the transition state. Furthermore, the formula can be implemented in the configuration space instead of the phase space integrals[24] to save the computational time for complex systems.

In this paper, we use this generalized NA-TST and the ZN theory coupled with quantum chemistry calculations to obtain the CT rates of quaterthiophene (4T) and sexithiophene (6T) single crystals. We focus on how the ET rates are changed with the electronic couplings as compared to those from the widely used semiclassical Marcus theory in organic material design. Figure 1 shows the crystal forms of 4T and 6T both of which have two molecules in each unit cell and have been obtained by Luciano *et al.*[33] and Siegrist *et al.*,[34] respectively. The choice of them, although arbitrary, is motivated by the fact that they have larger electronic couplings[35] than other oligothiophenes. Thus, it can be observed more obviously how the rates are deviated from those of the semiclassical Marcus formula with electronic couplings.

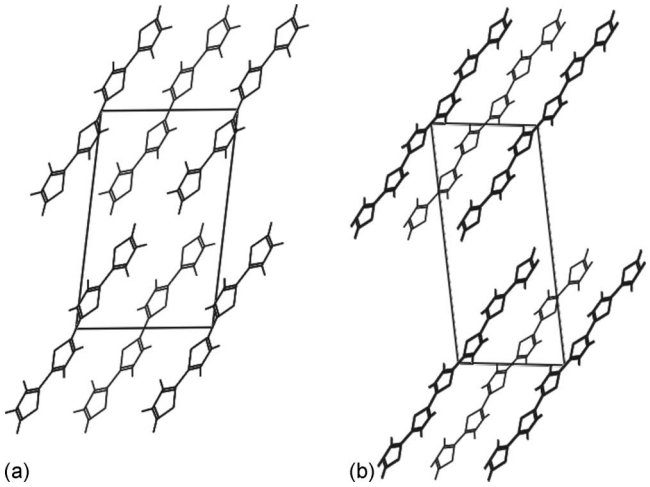

FIG. 1. The crystal forms of 4T and 6T along the unique axis (b). Left: the unit cell of 4T. Right: the unit cell of 6T.

This paper is arranged as follows: In Sec. II, we outline the theoretical background. Section III displays the numerical results and discussions. The conclusion is shown in Sec. IV.

II. METHODOLOGICAL APPROACH

A. Generalized nonadiabatic transition state theory

Starting from flux-side correlation function,[29] Zhao *et al.* derived a CT rate formula within the framework of the transition state theory,

$$k = \frac{k_B T}{h}\sqrt{\frac{\beta h^2}{2\pi}}\frac{Z^+}{Z_r} \times \frac{\int dQ P(\beta,Q)|\nabla(S(Q)-\xi_0)|\delta(S(Q)-\xi_0)e^{-\beta V_1(Q)}}{\int dQ|\nabla(S(Q)-\xi_0)|\delta(S(Q)-\xi_0)e^{-\beta V_1(Q)}}, \quad (2)$$

with an effective coordinate-dependent transition probability,

$$P(\beta,Q) = \beta\int_0^\infty dE_s e^{-\beta(E_s-V_1(Q))}P_{\mathrm{ZN}}(E_s,Q). \quad (3)$$

Here, E_s is the kinetic energy along the hopping direction, $P_{\mathrm{ZN}}(E_s,Q)$ is the ZN nonadiabatic transition probability[28] at given energy E_s, and Z^+ and Z^r are partition functions of the activated complex and the reactant, respectively.

In order to treat multidimensional systems, one has to employ the Monte Carlo approach to evaluate the integral in the configuration space. To do so, Eq. (1) is rewritten as

$$k = Z_{\mathrm{mod}} \sqrt{\frac{1}{2\pi\beta}} R_1 R_2, \tag{4}$$

with

$$R_1 = \frac{\int dQ e^{-\beta V_1(Q)} |\nabla(S(Q)-\xi_0)| \delta(S(Q)-\xi_0)}{\int d\xi \int dQ e^{-\beta V_1(Q)} |\nabla(S(Q)-\xi_0)| \delta(S(Q)-\xi)}, \tag{5}$$

$$R_2 = \frac{\int dQ e^{-\beta V_1(Q)} |\nabla(S(Q)-\xi_0)| \delta(S(Q)-\xi_0) P(\beta,Q)}{\int dQ e^{-\beta V_1(Q)} |\nabla(S(Q)-\xi_0)| \delta(S(Q)-\xi_0)} \tag{6}$$

and

$$Z_{\mathrm{mod}} = \frac{Z^+ Z_r^{\mathrm{cl}}}{Z_{\mathrm{cl}}^+ Z_r}, \tag{7}$$

where the index cl indicates that the corresponding quantities are evaluated classically, R_1 represents a ratio of the free energy on the seam surface and reactant partition function Z_{cl}, and R_2 is the thermal averaged nonadiabatic transition probability over the seam surface $S(Q)-\xi_0=0$. A simplified adaptive umbrella sampling approach[36] combined with the histogram technique has been used to simulate the R_1 and R_2-type integrals.

In the linear response limit, Eq. (4) can be cast to

$$k = \kappa k_{\mathrm{Marcus}}, \tag{8}$$

where k_{Marcus} is Eq. (1) and κ includes the effects of nonadiabatic transition and tunneling. At high temperature and weak electronic coupling limit, Eq. (8) can go back to Eq. (1). For the details of formula derivation and numerical simulations, one can see Refs. 30 and 31.

B. Computational approaches

We first recall that the λ in Eq. (1) includes the molecular geometry modifications that occur when an electron is added or removed from a molecule (inner reorganization), as well as the modifications in the surrounding medium due to polarization effects (outer reorganization). The latter is difficult to evaluate theoretically.[37] Here, we focus only on the intramolecular reorganization energy (λ_{in}) and its vibrational mode description.

Within the CT description picture for a molecule dimer M_1M_2, the initial state is represented as $|M_1^+M_2\rangle$ and the final state is $|M_1M_2^+\rangle$. The λ_{in} consists of two terms:[2,3] the relaxation energy of neutral molecule at the optimal charged molecular geometry (λ_1) and that of charged molecule at the optimized neutral molecular geometry (λ_2) (see Fig. 2). The λ_{in} can be evaluated in two ways: (i) directly from the adiabatic PESs of neutral and charged species;[38] or (ii) from the addition of each normal-mode relaxation energy as can be evaluated by the DUSHIN program developed by Reimers,[39]

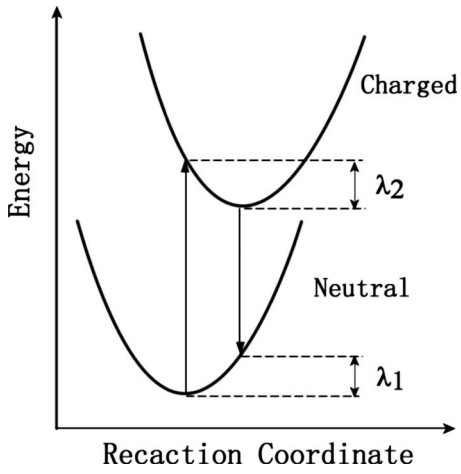

FIG. 2. Sketch of the PESs for neutral and cationic states, showing the vertical transitions and the relaxation energies λ_1 and λ_2.

which provides the partition of the λ_{in} into the contributions from each vibrational mode.

The geometric optimization and the normal-mode analysis of both 4T and 6T were carried out at the density functional theory (DFT) level by using the hybrid Becke's 3 parameters for exchange plus Lee-Yang-Parr's correlation functionals (B3LYP) with the 6-31G* basis set. All DFT calculations were performed with the GAUSSIAN 03 package.[40] It is found that the total reorganization energies by summing over the reorganization energies of the individual normal modes are 288.3 and 255.6 meV, respectively, for 4T and 6T. These values are very close to those by adiabatic potential approach, 285.7 and 243.5 meV. This shows that the harmonic oscillator approximation is excellent in describing the CT process in these molecules.

Having obtained the quantum modes, the Hamiltonians of reactants and products can be expressed as

$$H_1 = \sum_i \frac{P_i^2}{2} + V_1(Q) \tag{9}$$

and

$$H_2 = \sum_i \frac{P_i^2}{2} + V_2(Q), \tag{10}$$

with the PESs

$$V_1(Q) = \frac{1}{2}\sum_i \omega_i^2 Q_i^2 \tag{11}$$

and

$$V_2(Q) = \frac{1}{2}\sum_i \omega_i^2 (Q_i - Q_{0i})^2, \tag{12}$$

where

$$Q_{0i} = \frac{1}{\omega_i}\sqrt{2\lambda_i}. \tag{13}$$

The ω_i and λ_i are the frequency and reorganization energy of each mode. Then, the reaction coordinate ξ is defined as

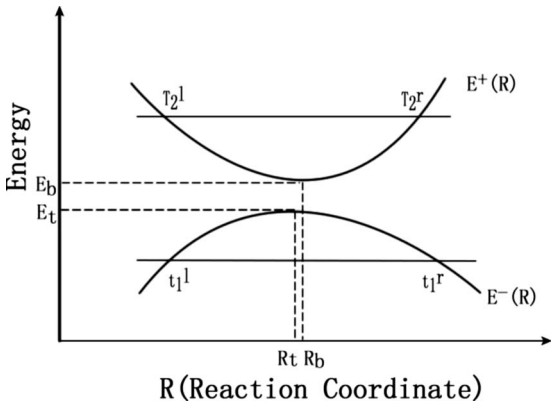

FIG. 3. Schematic two-state adiabatic potentials in the Marcus normal regime. Since the free energy difference ΔG is zero in our case, R_t should be equal to R_b.

$$\xi = V_1 - V_2 = \sum_i \left(\omega_i^2 Q_i Q_{0i} - \frac{1}{2}\omega_i^2 Q_{0i}^2 \right) \tag{14}$$

and the two adiabatic PESs are expressed as

$$E_{\pm}(Q) = \frac{1}{2}\{[V_1(Q) + V_2(Q)] \pm \sqrt{[V_1(Q) - V_2(Q)]^2 + 4t^2}\}, \tag{15}$$

which divide the whole energy into three regions ($E > E_b, E_b \geq E \geq E_t, E < E_t$) (see Fig. 3). E_t (E_b) is the maximum (minimum) point of the lower (upper) adiabatic potential surface, with R_t (R_b) as the corresponding reaction coordinate. t_1^l (T_2^l) and t_1^r (T_2^r) are the left and right reaction coordinates of each energy in the lower (upper) adiabatic potential. These parameters are required when ZN formulas are used in Eq. (3).

The next step is to calculate the electronic coupling term. Several methods have been proposed in the literature. The first one is the "energy splitting in dimer" (ESID) method,[7,41] which is based on Koopmans' theorem. In this case, the charge transfer integral corresponds to the half of the splitting of the highest occupied molecular orbital (HOMO) or lowest unoccupied molecular orbital levels for holes or electrons. Valeev *et al.*[42] cautioned recently that the transfer integral from dimer calculations cannot be reliably used to describe the extended systems and the site energy correction (SEC) due to the substantial polarization effects of the crystal environment should be taken into account. Li[43] advised that the electronic coupling can be obtained in the framework of transition state theory. The transition state needed to be determined, and the corresponding minimal energy splitting (MES) is twice of the transfer integral based on Koopmans' theorem. Another method is a direct method.[15,18,21] The electronic coupling can be obtained by directly evaluating the coupling element for the frontier orbitals.

In this paper, we adopt the direct method to obtain the electronic coupling. The reason for our choice can be seen below. Hartree–Fock (HF) bandwidth for a polymer has been shown to be always about 20%–30% larger than the result from (photoemission) experiments.[44] Moreover from previous studies, the electronic coupling from the DFT orbital is

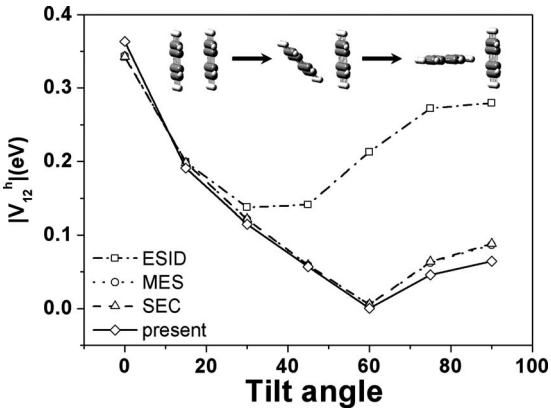

FIG. 4. Evolution of the hole transfer integral as a function of the tilt angle. The distance between a pair of pentacenes is $R = 3.5 + 1.5 \sin \gamma$. The dash dot line with square is the result from ESID approach; the dot line with circle shows the MES result; the dash line with triangle shows the SEC results; the solid line with diamond presents the result from the present direct method.

usually about 20% less than that of the HF orbital.[45] Thus, the Kohn–Sham–Fock operator is used instead of the HF operator to obtain the coupling in the framework of the DFT,[15,18,21]

$$V_{12}^h = \langle \phi_{\mathrm{HOMO}}^{0,\mathrm{site1}} | F | \phi_{\mathrm{HOMO}}^{0,\mathrm{site2}} \rangle, \tag{16}$$

where $\phi_{\mathrm{HOMO}}^{0,\mathrm{site1}}$ and $\phi_{\mathrm{HOMO}}^{0,\mathrm{site2}}$ are the HOMOs of the two adjacent molecules 1 and 2 when no intermolecular interaction is present. F is the Fock operator and its density matrix is constructed from noninteracting molecular orbitals:

$$F = SC\varepsilon C^{-1}. \tag{17}$$

Here, S is the intermolecular overlap matrix, C and ε are molecular orbital coefficients and energies from one-step diagonalization without iteration. The PW91 exchange and PW91 correlation functionals plus a 6-31G* basis set are employed. It has been shown that this choice can give the best description for electronic coupling at the DFT level.[46]

To show the reliability of this method, we have compared the dependence of the transfer integral as a function of the tilt angle γ from the above four methods. As an example, we take pentacene dimer, the transfer integral of which has been investigated by Valeev *et al.*[42] and our group.[15] It can be seen clearly in Fig. 4 that the ESID method[7,41] overestimates the electronic coupling when the two molecules of the dimer are inequivalent in the crystal. The polarization effect can lead to different site energies for inequivalent molecules in the crystal. However, the present direct method is almost identical to the SEC approach[42] and the MES approach[43] when the tilt angle is smaller than 60°. For larger tilt angles, the difference among them is still very little. Thus, we can believe that the direct method is reliable for the electronic coupling.

To better understand such consistency among these methods, some explanation is given below. The SEC approach obtains the orbitals from self-consistent iteration, so overlap corrections are required. Our direct method is in the spirit of first-order perturbation. Namely, it takes directly the unperturbed individual molecule's orbital and density matrix to guarantee that, originally, the two molecules are noninter-

acting, and only when putting them together can one get interaction information with respect to the individual molecules. However, the direct method is easier to perform than the former two methods. The SEC approach has to find the frontier orbital which may be difficult for large systems. The MES approach has to obtain all the energy splittings along the reaction coordinate to find the MES.

Having obtained the quantum modes and electronic coupling integrals, we can then calculate the CT rates in Eq. (4).

C. Random walk simulations for diffusion constant and mobility

Once the transfer rates have been obtained, we can then calculate the mobility by the Einstein formula: $\mu = eD/k_BT$. Here, the diffusion constant D is simulated by random walk.[21] First, one molecule is arbitrarily chosen as the starting point. The charge is only allowed to hop to the nearest neighbor molecules with a probability $p_\alpha = k_\alpha / \Sigma_\alpha k_\alpha$, where α is the hopping path. At each step, a random number r is uniformly generated between 0 and 1. If $\Sigma_\alpha^{j-1} p_\alpha < r \leq \Sigma_\alpha^{j} p_\alpha$, the charge then goes to the neighbor in the jth direction as the next position of the charge. The simulation time is chosen to be 10 μs, and the diffusion constant is obtained by $D = \lim_{t\to\infty} l(t)^2/6t$ where $l(t)^2$ is the mean squared displacement. Two thousand simulations are performed to get a converged diffusion constant.

In order to estimate the statistics error for mobility, one would sort to carry out many times such processes each of which contains 2000 simulations. This would be very time consuming. Here, we adopt a simpler sampling approach, which has been shown to be both very efficient and very effective.[21] Here is what we do. The 2000 results of mobility obtained from simulation are large enough. Each result is regarded as a point. We randomly select one point out of the 2000 for 2000 times. Then we will have another set of 2000 points. Note that the same points could be selected several times because each selection is independent. We find that when such random process is done for 100 times, the final result is close to that of 200 000 simulations.[21] Namely, now we have 100 sets, each of which contains 2000 points. The statistical error of mobility is then estimated by $\frac{1}{2}\max\{\mu_i\} - \frac{1}{2}\min\{\mu_i\}$.

III. RESULTS AND DISCUSSION

Figure 5 shows several different types of dimers in the 4T and 6T single crystals. The corresponding transfer integrals of the nearest neighbors are listed in Table I. The rates from FGR (Refs. 20 and 21) have also been displayed to make connection between the GNTST and the semiclassical Marcus formulas. The relationship among them is described in the following:

$$\text{GNTST} \xrightarrow[\text{coupling}]{\text{weak}} \text{FGR} \xrightarrow[\text{temperature}]{\text{high}} \text{Marcus}.$$

The results for 4T single crystals are shown in Fig. 6. Four representative dimers have been chosen, which cover from the weakest to the strongest electronic couplings. We first compare the rates from the semiclassical Marcus and

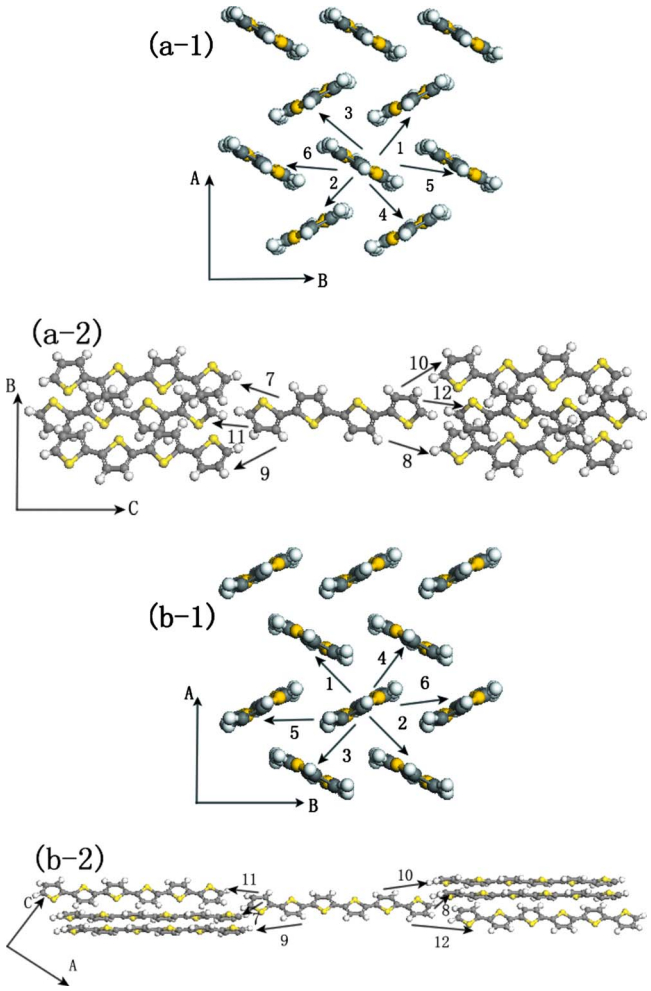

FIG. 5. (Color online) The chosen nearest neighbors in the 4T and 6T single crystals: (a) for 4T; (b) for 6T. (a)(1) and (b)(1) correspond to the pathways in the same layers; (a2) and (b2) are the hopping routes in the different layers.

FGR treatments. It can be seen in Fig. 6 that the Marcus rates are much lower than the FGR rates at the room temperature for various electronic couplings, but the former gradually approach the latter with the temperature and become nearly

TABLE I. Transfer integrals of the nearest neighbors in 4T and 6T single crystals at DFT level with PW91 exchange and PW91 correlation functionals plus a 6-31G* basis set.

Dimers	4T (meV)	6T (meV)
1	39.95	36.00
2	39.94	36.08
3	39.81	36.06
4	39.79	36.14
5	4.45	3.37
6	4.45	3.37
7	2.36	0.72
8	2.36	0.73
9	2.35	0.73
10	2.34	0.73
11	0.68	0.38
12	0.68	0.38

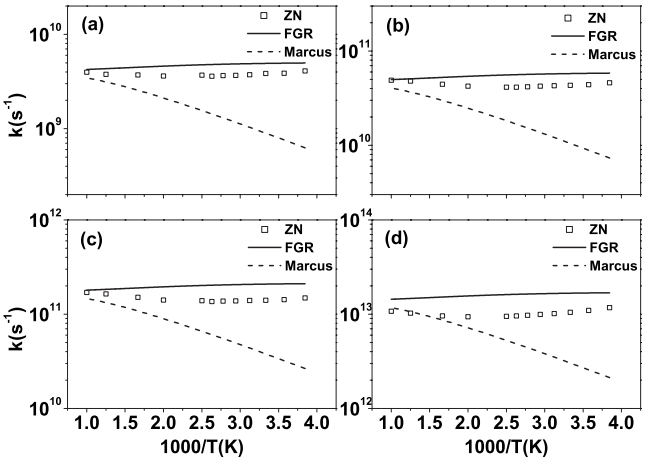

FIG. 6. Arrhenius plots of the CT rates for various electronic couplings in 4T single crystal as listed in Table I: (a) for dimer 11; (b) for dimer 10; (c) for dimer 6; (d) for dimer 4. The square represents the GNTST results; the solid line represents the FGR results; the dashed line represents the Marcus results.

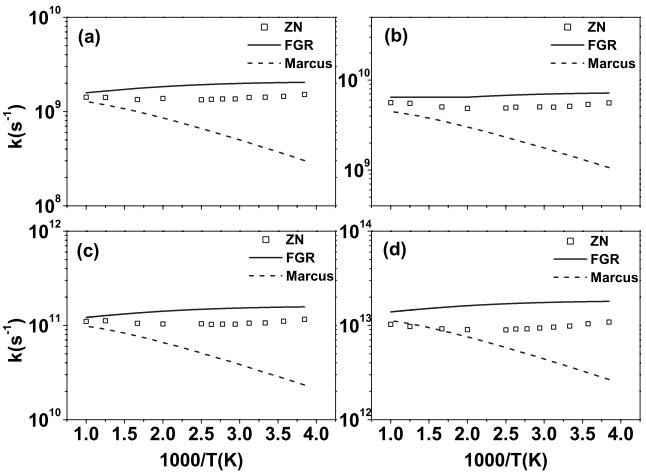

FIG. 7. Arrhenius plots of the CT rates for various electronic couplings in 6T single crystal as listed in Table I: (a) for dimer 11; (b) for dimer 7; (c) for dimer 6; (d) for dimer 1. The symbols are the same as in Fig. 6.

identical to the latter when the temperature reaches 1000 K. This is attributed to the fact that the semiclassical Marcus theory is in the classical regime—that is, $\hbar\omega_j/k_bT \ll 1$. Although the actual crystals cannot exist in such high temperature, it is still meaningful to comprehend the applicable condition of different formulas from the theoretical standpoint. For the FGR and GNTST treatments, it is obvious that the GNTST rates are almost consistent with those from the FGR treatment as expected when the transfer integral is smaller than 5 meV. However, the GNTST results become smaller than those of the FGR when the electronic coupling comes to about 40 meV. Thus, the perturbation theory in the strong electronic coupling regime predicts incorrect transfer rates. Based on the above discussion, we can see in Fig. 6 that the GNTST formula predicts more than three times larger rates than the semiclassical Marcus formula at the room temperature. Furthermore, both formulas predict nearly identical results for the strongest electronic coupling when the temperature is close to 600 K and the GNTST begins to show slightly smaller rates than those from the Marcus prediction.

The transfer rates for 6T have been shown in Fig. 7. Since 4T and 6T have similar molecular conjugate structure and crystal stack, the overall tendency is similar in Fig. 7 as in Fig. 6.

Figure 8 shows the relationship between the CT rates and the electronic couplings for 4T and 6T. As mentioned above, the nuclear tunneling is excluded in the semiclassical Marcus formula, so that the Marcus rates are consistently smaller than the FGR rates. Compared to the GNTST prediction of 4T, we can see in Fig. 8(a) that the GNTST rates are nearly consistent with the rates from the FGR treatment when the electronic coupling is smaller than 10 meV. This exhibits the perturbation regime of the electronic couplings for 4T. As the electronic couplings increase, the GNTST rates are gradually smaller than the FGR rates and become almost identical to the Marcus rates at about 40 meV. As we pointed out previously, there are two things missing in the semiclassical Marcus theory—quantum nuclear tunneling and nonperturbation. The former tends to enhance, while the latter tends to reduce the rate from the semiclassical Marcus theory. Our GNTST rate contains both contributions. Thus, it is just an accidental coincidence that at $V=40$ meV, the rates from our GNTST is close to that from the semiclassical Marcus theory. For 6T, it is obvious in Fig. 8(b) that the perturbation regime of the electronic couplings is reduced to 5 meV. This is because 6T has smaller reorganization than 4T.

At this stage, it should be mentioned that there are other derivations made by Bixon and Jortner[47] where intramolecular modes are treated at the quantum mechanical level. While it has the same first-order perturbative nature as the FGR treatment, the Bixon–Jortner model is a further simplification of FGR for one or two effective vibrational modes (harmonic oscillators). FGR and GNTST we used in this work have considered all the intramolecular normal modes. In addition, we have tried the Bixon–Jortner way for the transport properties, and we find that the way to define one or two effective modes is quite arbitrary.

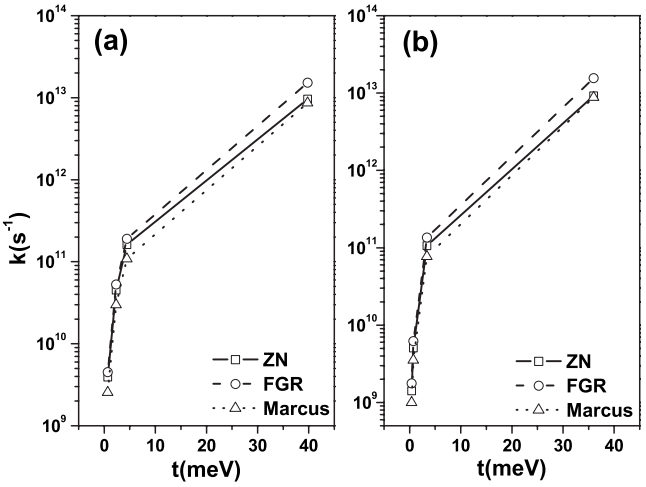

FIG. 8. The CT rates vs electronic coupling strengths of the 4T and 6T single crystal at 600 K. The solid line with square shows the GNTST results; the dashed line with circle shows the results from the FGR treatment; the dotted line with triangle shows the results from the semiclassical Marcus formula.

With the GNTST rates, the room temperature mobilities for 4T and 6T are 0.066 ± 0.004 and 0.067 ± 0.004 $cm^2/V\,s$, respectively. Note that our previous simulation based on the semiclassical Marcus theory gave 0.021 ± 0.0011 and 0.026 ± 0.0013 $cm^2/V\,s$.[48] Namely, the combined effect of nuclear tunneling and nonperturbative effects result in a mobility about three times as large as that from the semiclassical Marcus theory. The reported measurements of mobilities in oligothiophene thin films are in the range of $0.002-0.2$ $cm^2/V\,s$,[49] which is not precise enough to verify the theoretical results.

IV. CONCLUSION

In this work, we have obtained the CT rates of 4T and 6T single crystals with a generalized NA-TST which applies to any electronic couplings. The nuclear tunneling effect has also been properly included into the prefactor of Eq. (8). Our calculation shows that the CT rates are no longer proportional to the square of the electronic couplings as the case for the FGR treatment, but become gradually smaller than the latter with the electronic couplings. Due to the nuclear tunneling contribution, the GNTST results are obviously larger than the Marcus results at 300 K, and become nearly identical with the Marcus results when the temperature is increased to 600 K. We thus propose the GNTST as a more general quantum chemistry approach for designing organic semiconductors. For the oligothiophene, the GNTST-calculated hole mobility is about three times as large as that from the semiclassical Marcus theory.

ACKNOWLEDGMENTS

This work was supported by the Ministry of Science and Technology of China (Grant Nos. 2006CB806200, 2006CB0N0100, and 2009CB623600), and NSFC (Grant No. 20833004).

[1] R. G. Kepler, P. E. Bierstedt, and R. E. Merrifeld, Phys. Rev. Lett. **5**, 503 (1960); F. Gutman and L. E. Lyons, *Organic Semiconductors* (Wiley, New York, 1967); W. Mey, T. J. Sonnonstine, D. L. Morel, and A. M. Hermann, J. Chem. Phys. **58**, 2542 (1973).
[2] M. Pope and C. E. Swenberg, *Electronic Processes in Organic Crystals and Polymers*, 2nd ed. (Oxford University Press, New York, 1999).
[3] E. A. Silinsh and V. Capek, *Organic Molecular Crystals: Interaction, Localization, and Transport Phenomena* (AIP, New York, 1994).
[4] M. E. Gershenson, V. Podzorov, and A. F. Morpurgo, Rev. Mod. Phys. **78**, 973 (2006); S. Günes, H. Neugebauer, and N. S. Sariciftci, Chem. Rev. (Washington, D.C.) **107**, 1324 (2007).
[5] J. L. Brédas, J. P. Calbert, D. A. da Silva Filho, and J. Cornil, Proc. Natl. Acad. Sci. U.S.A. **99**, 5804 (2002).
[6] A. J. Epstein, W. P. Lee, and V. N. Prigodin, Synth. Met. **117**, 9 (2001).
[7] (a) G. R. Hutchison, M. A. Ratner, and T. J. Marks, J. Am. Chem. Soc. **127**, 16866 (2005); (b) N. Karl, Synth. Met. **133–134**, 649 (2003); (c) L. J. Wang, Q. Peng, Q. K. Li, and Z. Shuai, J. Chem. Phys. **127**, 044506 (2007); (d) K. Hannewald and P. A. Bobbert, Appl. Phys. Lett. **85**, 1535 (2004); (e) V. Podzorov, E. Menard, J. A. Rogers, and M. E. Gershenson, Phys. Rev. Lett. **95**, 226601 (2005).
[8] (a) O. D. Jurchescu, J. Baas, and T. T. M. Palstra, Appl. Phys. Lett. **84**, 3061 (2004); (b) H. Klauk, D. J. Gundlach, J. A. Nichols, and T. N. Jackson, IEEE Trans. Electron Devices **46**, 1258 (1999).
[9] D. A. da Silva Filho, E. G. Kim, and J. L. Brédas, Adv. Mater. (Weinheim, Ger.) **17**, 1072 (2005).
[10] S. Nagamatsu, K. Kaneto, R. Azumi, M. Matsumoto, Y. J. Yoshida, and K. Yase, J. Phys. Chem. B **109**, 9374 (2005); M. Melucci, M. Gazzano, G. Barbarella, M. Cavallini, F. Biscarini, P. Maccagnani, and P. Ostoja, J. Am. Chem. Soc. **125**, 10266 (2003); X. M. Hong, H. E. Katz, A. J. Lovinger, B. C. Wang, and K. Raghavachari, Chem. Mater. **13**, 4686 (2001); M. E. Hajlaoui, F. Garnier, L. Hassine, F. Kouki, and H. Bouchriha, Synth. Met. **129**, 215 (2002).
[11] Y. C. Cheng, R. J. Silbey, D. A. da Silva Filho, J. P. Calbert, J. Cornil, and J. L. Brédas, J. Chem. Phys. **118**, 3764 (2003).
[12] G. Horowitz, R. Hajlaoui, R. Bourguiga, and M. Hajlaoui, Synth. Met. **101**, 401 (1999).
[13] R. A. Marcus, Rev. Mod. Phys. **65**, 599 (1993).
[14] Y. A. Berlin, G. R. Hutchison, P. Rempala, M. A. Ratner, and J. Michl, J. Phys. Chem. A **107**, 3970 (2003); W. Q. Deng and W. A. Goddard III, J. Phys. Chem. B **108**, 8614 (2004); Y. B. Song, C. A. Di, X. D. Yang, S. P. Li, W. Xu, Y. Q. Liu, L. M. Yang, Z. G. Shuai, D. Q. Zhang, and D. B. Zhu, J. Am. Chem. Soc. **128**, 15940 (2006).
[15] (a) X. D. Yang, Q. K. Li, and Z. Shuai, Nanotechnology **18**, 424029 (2007); (b) S. W. Yin, Y. P. Yi, Q. X. Li, G. Yu, Y. Q. Liu, and Z. G. Shuai, J. Phys. Chem. A **110**, 7138 (2006).
[16] O. Ostroverkhova, D. G. Cooke, F. A. Hegmann, J. E. Anthony, V. Podzorov, M. E. Gershenson, O. D. Jurchescu, and T. T. M. Palstra, Appl. Phys. Lett. **88**, 162101 (2006); V. Podzorov, E. Menard, A. Borissov, V. Kiryukhin, J. A. Rogers, and M. E. Gershenson, Phys. Rev. Lett. **93**, 086602 (2004); V. Podzorov, E. Menard, J. A. Rogers, and M. E. Gershenson, *ibid.* **95**, 226601 (2005).
[17] V. M. Kenkre, Phys. Lett. A **305**, 443 (2002); P. J. Brown, H. Sirringhaus, M. Harrison, M. Shkunov, and R. H. Friend, Phys. Rev. B **63**, 125204 (2001).
[18] A. Troisi and G. Orlandi, Chem. Phys. Lett. **344**, 509 (2001).
[19] A. Troisi and G. Orlandi, J. Phys. Chem. A **110**, 4065 (2006); A. Troisi and G. Orlandi, Phys. Rev. Lett. **96**, 086601 (2006); A. Troisi, Adv. Mater. (Weinheim, Ger.) **19**, 2000 (2007).
[20] S. H. Lin, C. H. Chang, K. K. Liang, R. Chang, J. M. Zhang, T. S. Yang, M. Hayashi, Y. J. Shiu, and F. C. Hsu, Adv. Chem. Phys. **121**, 1 (2002).
[21] G. J. Nan, X. D. Yang, L. J. Wang, Z. Shuai, and Y. Zhao (unpublished).
[22] P. Hänggi, P. Talkner, and M. Borkovec, Rev. Mod. Phys. **62**, 251 (1990).
[23] A. J. Leggett, S. Chakravarty, A. T. Dorsey, M. P. A. Fisher, A. Garg, and W. Zwerger, Rev. Mod. Phys. **59**, 1 (1987).
[24] G. E. Zahr, R. K. Preston, and W. H. Miller, J. Chem. Phys. **62**, 1127 (1975); E. J. Heller and R. C. Brown, *ibid.* **79**, 3336 (1983); A. J. Marks and D. L. Thompson, *ibid.* **96**, 1911 (1992); A. J. Marks, *ibid.* **114**, 1700 (2001); M. S. Topaler and D. G. Truhlar, *ibid.* **107**, 392 (1997).
[25] F. Remacle, D. Dehareng, and J. C. Lorquet, J. Phys. Chem. **92**, 4784 (1988); Q. Cui, K. Morokuma, and J. M. Bowman, J. Chem. Phys. **110**, 9469 (1999).
[26] J. C. Lorquet and B. Leyh-Nihant, J. Phys. Chem. **92**, 4778 (1988).
[27] L. Landau, Phys. Z. Sowjetunion **2**, 46 (1932); C. Zener, Proc. R. Soc. London, Ser. A **137**, 696 (1932).
[28] C. Zhu and H. Nakamura, J. Chem. Phys. **101**, 10630 (1994); C. Zhu and H. Nakamura, *ibid.* **108**, 7501 (1998); C. Zhu, Y. Teranishi, and H. Nakamura, Adv. Chem. Phys. **117**, 127 (2001).
[29] W. H. Miller, S. D. Schwartz, and J. W. Tromp, J. Chem. Phys. **79**, 4889 (1983).
[30] Y. Zhao, G. Mil'nikov, and H. Nakamura, J. Chem. Phys. **121**, 8854 (2004).
[31] Y. Zhao, W. Z. Liang, and H. Nakamura, J. Phys. Chem. A **110**, 8204 (2006).
[32] Y. Zhao, X. Li, Z. L. Zheng, and W. Z. Liang, J. Chem. Phys. **124**, 114508 (2006).
[33] L. Antolini, H. Gilles, K. Faycal, and G. Francis, Adv. Mater. (Weinheim, Ger.) **10**, 382 (1998).
[34] T. Siegrist, R. M. Fleming, R. C. Haddon, R. A. Laudise, A. J. Lovinger, H. E. Katz, P. Bridenbaugh, and D. D. Davis, J. Mater. Res. **10**, 2170 (1995).
[35] T. Siegrist, C. Kloc, R. A. Laudise, H. E. Katz, and R. C. Haddon, Adv. Mater. (Weinheim, Ger.) **10**, 379 (1998); R. C. Haddon, T. Siegrist, R. M. Fleming, P. M. Bridenbaugh, and R. A. Laudise, J. Mater. Chem. **5**, 1719 (1995).
[36] T. Yamamoto and W. H. Miller, J. Chem. Phys. **120**, 3086 (2004); Y. Zhao, T. Yamamoto, and W. H. Miller, *ibid.* **120**, 3100 (2004).
[37] E. V. Tsiper and Z. G. Soos, Phys. Rev. B **68**, 085301 (2003); E. V. Tsiper, Z. G. Soos, W. Gao, and A. Kahn, Chem. Phys. Lett. **360**, 47 (2002).
[38] M. Malagoli and J. L. Brédas, Chem. Phys. Lett. **327**, 13 (2000).
[39] J. R. Reimers, J. Chem. Phys. **115**, 9103 (2001).
[40] M. J. Frisch, G. W. Trucks, H. B. Schlegel *et al.*, GAUSSIAN 03, Revision

A. 1, Gaussian, Inc., Pittsburgh PA, 2003.
[41] J. Cornil, D. Beljonne, J. P. Calbert, and J. L. Brédas, Adv. Mater. (Weinheim, Ger.) **13**, 1053 (2001).
[42] E. F. Valeev, V. Coropceanu, D. A. da Silva Filho, S. Salman, and J. L. Brédas, J. Am. Chem. Soc. **128**, 9882 (2006).
[43] X. Y. Li, J. Comput. Chem. **22**, 565 (2001).
[44] J. M. André, J. Delhalle, and J. L. Brédas, *Quantum Chemistry Aided Design of Organic Polymers: An Introduction to the Quantum Chemistry of Polymers and its Applications* (World Scientific, Singapore, 1991).
[45] C. J. Calzado and J. P. Malrieu, Chem. Phys. Lett. **317**, 404 (2000).
[46] J. S. Huang and M. Kertesz, Chem. Phys. Lett. **390**, 110 (2004).
[47] M. Bixon and J. Jortner, J. Phys. Chem. **95**, 1941 (1991).
[48] X. D. Yang, L. J. Wang, C. L. Wang, W. Long, and Z. G. Shuai, Chem. Mater. **20**, 3205 (2008).
[49] R. Hajlaoui, G. Horowitz, F. Garnier, A. A. Brouchet, L. Laigre, A. E. Kassmi, F. Demanze, and F. Kouki, Adv. Mater. (Weinheim, Ger.) **9**, 389 (1997); G. Horowitz, *ibid.* **10**, 365 (1998); G. Horowitz and M. E. Hajlaoui, *ibid.* **12**, 1046 (2000); G. Horowitz, M. E. Hajlaoui, and R. Hajlaoui, J. Appl. Phys. **87**, 4456 (2000); M. Halik, H. Klauk, U. Zschieschang, G. Schmid, S. Ponomarenko, S. Kirchmeyer, and W. Weber, Adv. Mater. (Weinmheim, Ger.) **15**, 917 (2003); S. Nagamatsu, K. Kaneto, R. Azumi, M. Matsumoto, Y. Yoshida, and K. Yase, J. Phys. Chem. B **109**, 9374 (2005).